



Publication Year	2015
Acceptance in OA	2021-04-26T13:22:42Z
Title	First INTEGRAL Observations of V404 Cygni during the 2015 Outburst: Spectral Behavior in the 20-650 keV Energy Range
Authors	Roques, Jean-Pierre, Jourdain, Elisabeth, BAZZANO, ANGELA, FIOCCHI, MARIATERESA, NATALUCCI, LORENZO, UBERTINI, PIETRO
Publisher's version (DOI)	10.1088/2041-8205/813/1/L22
Handle	http://hdl.handle.net/20.500.12386/30916
Journal	THE ASTROPHYSICAL JOURNAL LETTERS
Volume	813

FIRST *INTEGRAL* OBSERVATIONS OF V404 CYGNI DURING THE 2015 OUTBURST: SPECTRAL BEHAVIOR IN THE 20–650 KeV ENERGY RANGE*

JEAN-PIERRE ROQUES¹, ELISABETH JOURDAIN¹, ANGELA BAZZANO², MARIATERESA FIOCCHI²,
LORENZO NATALUCCI², AND PIETRO UBERTINI²

¹ Université Toulouse, UPS-OMP, CNRS, IRAP, 9 Av. Roche, BP 44346, F-31028 Toulouse, France

² Istituto di Astrofisica e Planetologia Spaziali, INAF, Via Fosso del Cavaliere 100, I-00133 Roma, Italy

Received 2015 August 12; accepted 2015 October 9; published 2015 October 30

ABSTRACT

In 2015 June, the source V404 Cygni (= GS2023+38) underwent an extraordinary outburst. We present the results obtained during the first revolution dedicated to this target by the *INTEGRAL* mission and focus on the spectral behavior in the hard X-ray domain, using both SPI and IBIS instruments. The source exhibits extreme variability and reaches fluxes of several tens of Crab. However, the emission between 20 and 650 keV can be understood in terms of two main components, varying on all the observable timescales, similar to what is observed in the persistent black hole system Cyg X-1. The low-energy component (up to ~ 200 keV) presents a rather unusual shape, probably due to the intrinsic source variability. Nonetheless, a satisfactory description is obtained with a Comptonization model, if an unusually hot population of seed photons ($kT_0 \sim 7$ keV) is introduced. Above this first component, a clear excess extending up to 400–600 keV leads us to investigate a scenario where an additional (cutoff) power law could correspond to the contribution of the jet synchrotron emission, as proposed in Cyg X-1. A search for an annihilation feature did not provide any firm detection, with an upper limit of 2×10^{-4} ph cm⁻² s⁻¹ (2σ) for a narrow line centered at 511 keV, on the averaged obtained spectrum.

Key words: black hole physics – gamma-ray burst: individual (V404 Cygni = GS2023+338) – radiation mechanisms: general – X-rays: binaries

1. INTRODUCTION

The 2015 outburst of V404 Cyg will probably remain a unique event in astrophysical history. Identified as a nova in 1938, when only optical observations were available, V404 Cyg came back to the forefront in 1989 when another nova episode was observed simultaneously in the optical and in the soft X-ray and hard X-ray domains by the *GINGA* satellite (from where its second name comes from, GS2023+338; Makino 1989) and the Roentgen instruments on board the Kvant module (Syunyaev et al. 1991). It presented huge variability and reached several Crab flux levels, in soft X-rays as well as in hard X-rays, becoming the brightest source ever observed in these energy ranges. The parameters have been determined, with the system located at 2.39 ± 0.14 kpc (Miller-Jones et al. 2009) and containing a $\sim 10 M_\odot$ black hole, with an orbital period around 6.5 days (Casares et al. 1992). The 2015 episode started with similar burst-like activity that was first detected by *Swift*/BAT (Barthelmy et al. 2015) and *Fermi*/GBM (Younes 2015), and soon after was observed at all wavelengths from radio (Mooley et al. 2015) to hard X-rays and reached exceptional levels of luminosity, exceeding all expectations (up to 50 Crab in hard X-rays; Rodriguez et al. 2015).

Among the global monitoring of the source, *INTEGRAL*, with its two main instruments SPI and IBIS, played a major role in the hard X-ray/soft γ -ray studies.

2. INSTRUMENT, OBSERVATIONS, AND DATA ANALYSIS

We analyzed the first public observation from 2015 June 17 to 20 (revolution 1554) for a total useful duration of 150 ks. The SPI analysis is based on consolidated data and algorithms developed at IRAP.³ Considering the source exceptional flux level and variability, it is worth mentioning that the SPI data are not affected by pile-up or TM saturation. Only a limited number of data packets are missing corresponding to a few seconds of data, with an energy independent effect. The IBIS data for this observation are near real-time data processed using the latest release of the *INTEGRAL* Offline Scientific Analysis (OSA version 10.1). The IBIS and SPI results have been compared and show that the source fluxes are in good agreement, even if at high flux levels, IBIS/ISGRI spectra appear systematically harder than the SPI ones (see analysis by Natalucci et al. 2015). The reason for this is under investigation and is probably related to a combination of source variability and telemetry saturation. The description of the instruments and performance can be found in Vedrenne et al. (2003) and Roques et al. (2003) for SPI and Ubertini et al. (2003) for IBIS.

3. BROADBAND AND SPECTRAL EVOLUTION

The source variability at all wavelengths and on all timescales is striking. However, the emission above ~ 200 keV contains key information about the population(s) present and energy transfer but requires longer integration time. The present analysis is based on the science window (scw) timescale, a time interval lasting approximately 3.4 ks and

* Based on observations with *INTEGRAL*, an ESA project with instruments and science data center funded by ESA member states (especially the PI countries: Denmark, France, Germany, Italy, Spain, and Switzerland), Czech Republic, and Poland with the participation of Russia and USA.

³ An open SPI Data Analysis Interface (*SPIDAI*) allows one to perform the SPI data analysis with the same tools as those used in this Letter. See the dedicated webpage <http://sigma-2.cesr.fr/integral/spidai>.

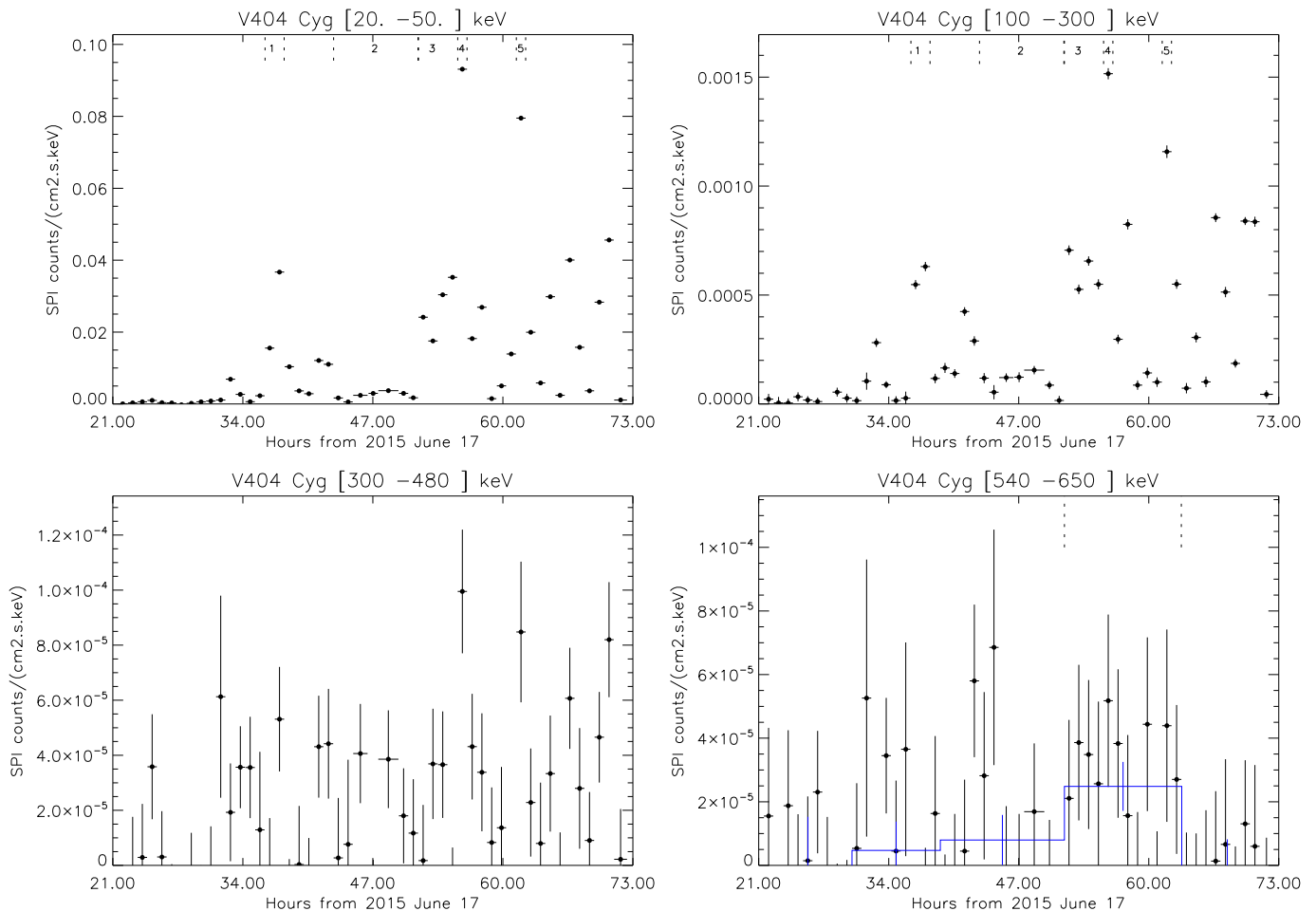


Figure 1. SPI light curves of V404 Cyg from June 17 to 20 on the scw timescale (~ 1 hr). In the last panel, the blue histogram corresponds to an ~ 10 hr timescale.

corresponding to a stable pointing direction. Figure 1 displays the source evolution over four broad bands covering the 20–650 keV domain and demonstrates that on this approximately hour timescale, the source variability is significant up to ~ 500 keV and appears energy dependent.

In order to quantify the spectral evolution, the observed emission is described with a common model, both physically reasonable and as simple as possible. An averaged spectrum has been built and fitted with the `xSPEC` (v12.8.2) tools (Arnaud 1996). Starting from a Comptonization model, we note the emergence of a high-energy component around 100 keV. This component is reminiscent of the hard tail observed in several X-ray binary systems, transient sources (e.g., Nova Persei = GROJ0422+32; Roques et al. 1994) or persistent sources (e.g., Cyg X-1). Continuing the analogy with the well-studied source Cyg X-1, we add to our model the same second component (cutoff power law) used to account for the high-energy tail in the hard state. This simple model failed to take into account the actual curvature in the low-energy part, and we have tested a scenario with a reflecting and/or absorbing medium. The required values imply very specific geometry or a strong absorption of photons at lower energy. As a second option, we relaxed the constraint on the temperature of seed photons (kT_0). Surprisingly, a temperature around 6–7 keV perfectly reproduces the data.

Finally, we have chosen to describe the spectral emission of V404 Cyg with the following model: a Comptonization

component (Comptt), with two free parameters (kT and τ , temperature and optical depth of the Comptonizing electron population, with kT_0 fixed to 6.5 or 7 keV; see Table 1) and a cutoff power law, to account for the high-energy part. We fix its photon index to 1.6 and start with a cutoff energy default value of 300 keV.

From Figure 1, a few periods have been chosen to illustrate the spectral evolution of V404 Cyg:

1. First small peak (June 18, 12:11–14:07 UT; 6 ks);
2. “Off-flare” state (June 18, 19:02–June 19, 03:29 UT; 25 ks);
3. Plateau (June 19, 03:31–07:25 UT; 11.5 ks);
4. First maximum peak (June 19, 07:26–08:23 UT; 3 ks); and
5. Second maximum peak (June 19, 13:19–14:15 UT; 3 ks).

The corresponding spectra are compared in Figure 2. Table 1 gives the best-fit parameter values when they are fit individually and the parameters obtained for the averaged spectrum for comparison. For the low flux periods ([1] and [2]), the cutoff power-law component is not required, probably due to the low signal-to-noise ratio. Note that these periods are described by a hotter and thinner Comptonizing medium, while the temperature decreases and the optical depth increases when the source’s flux is high. In a second step, to overcome the error bars and degeneracy between kT and τ , we have also fit all the spectra together, aiming to extract more information with a

Table 1
Best-fit Parameters for Individual Spectra (Comptt + Cutoff Power-law Model)

Spectrum Label	kT (keV)	τ	$F_{[25-100 \text{ keV}]}$ ^a ($10^{-2} \text{ ph cm}^{-2} \text{ s}$)	E_{cut} (keV)	$N_{[1 \text{ keV}]}$ ^b ($\text{ph cm}^{-2} \text{ s keV}$)	χ_{red}^2 (dof)
Averaged spectrum	26.4 ± 2	1.6 ± 0.2	26.0 ± 0.9	241 ± 40	1.4 ± 0.02	1.1 (35)
First small peak [1] (scw 19–20)	42 ± 5	1.1 ± 0.2	43 ± 2.4	not required	...	1.1 (36)
“Off-flare” [2] (scw 26–32)	53^{+44}_{-12}	1.2 ± 0.5	5.7 ± 1.2	not required	...	1.2 (34)
Plateau [3] (scw 33–36)	28 ± 3	1.6 ± 0.2	50.5 ± 4	296 ± 80	1.7	1.4 (35)
First Maximum (scw 37) [4]	21 ± 2	1.9 ± 0.2	174 ± 6	189^{+74}_{-36}	8 ± 1.6	1.23 (35)
2nd Maximum (scw 43) [5]	23 ± 2	1.7 ± 0.2	156 ± 7	189 ± 40	5.4 ± 1.8	1.0 (35)
		==	common fit	==		
Averaged spectrum	27.8 ± 1	1.55 ± 0.1	25.9 ± 0.3	242 ± 20	1.3 ± 0.03	1.2 (37)
First small peak [1] (scw 19–20)	”	”	42.5 ± 1.2	300 (fix)	1.9 ± 0.1	1.1 (38)
“Off-flare” [2] (scw 26–32)	43 ± 4	”	4.9 ± 1.3	”	0.2 ± 0.1	1.2 (34)
Plateau [3] (scw 33–36)	idem [1]	”	50 ± 1.3	”	1.8 ± 0.07	1.3 (38)
Maximum (scw 37) [4]	25 ± 1	”	183.8 ± 1.8	”	4.3 ± 0.15	1.3 (38)
2nd Maximum (scw 43) [5]	”	”	164.4 ± 1.9	”	2.6 ± 0.16	1.4 (38)
		==	100 s timescale	==		
100 s Max bin [6]	22.5 ± 1	1.55 (fix)	680 ± 12	300 (fix)	9.8 ± 1	0.93 (36)

Notes. Parameters obtained for the individual spectra displayed in Figure 2. Top: each spectrum is fit individually. Bottom: spectra are fit simultaneously, with some parameters forced to be equal to have the minimum of free parameters. The kT_0 is fixed to 7 keV, except for [1], which requires a value of 6.5 keV. Photon index of the cutoff power-law component is fixed to 1.6.

^a For the Comptonization component.

^b Cutoff power-law normalization at 1 keV.

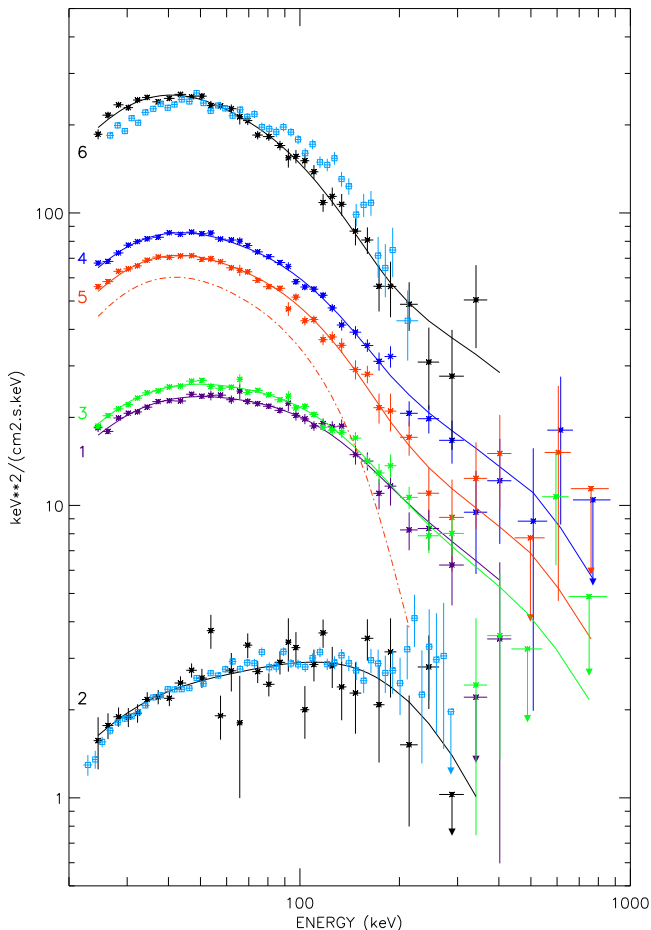


Figure 2. Evolution of the spectral shape of V404 Cyg on the 1–4 hr (labels 1–5) and 100 s (label 6) timescales. Crosses correspond to SPI data, and open squares to IBIS/ISGR1 data (for labels 2 and 6 only). Solid lines are the best common fit models, given in Table 1. See the text for the period definition.

minimal number of free parameters. We thus started our fitting procedure by imposing the same parameter values (except normalizations) to all considered spectra and freed successively, one by one, those required to improve significantly the global χ^2 . Finally (see Table 1), a global reasonable description is obtained with kT_0 fixed to 7.0 keV and photon index to 1.6, while a common τ converges toward a value of 1.55. The cutoff energy is fixed to 300 keV for all spectra, but the averaged one. Because the average spectrum includes a lot of spectral variability, its scientific content is limited. The most striking result is that, in such a scheme, the temperature is stable (between 25 and 28 keV), except during the period where the source seems to be less active (period [2]). The spectral emission at that time is harder, and this translates into a Comptonizing temperature of 40–50 keV. It is worth noting that the high-energy component is formally required in the high-flux-level spectra and that introducing it in the moderate-flux peak (period [1]) affects the best-fit parameters in such a way that they become compatible with those obtained during the high-flux periods (see Table 1). Note also that at shorter timescales, the spectral shape evolution can be described with the same scheme. In Figure 2, spectrum [6] corresponds to the maximum in a 100 s time bin. When this short spectrum is compared to the longer-term spectra, the global shapes appear similar, indicating that low- and high-energy components evolve more or less in the same way at all timescales. This information, together with correlations at other wavelengths, will be crucial for drawing a more complete picture of the emitting regions and their intrinsic evolution.

As a supplementary study, we have considered a 4.5 keV wide channel centered at 511 keV in order to search for an annihilation emission. The observed flux remains below 2σ for each of the individual scws, leading to an upper limit of $(1-2) \times 10^{-3} \text{ ph cm}^{-2} \text{ s}^{-1}$. When considering the whole revolution (150 ks), we obtain a 2σ upper limit of

$2 \times 10^{-4} \text{ ph cm}^{-2} \text{ s}^{-1}$. Compared to the values given for other black hole binaries in Teegarden & Watanabe (2006), these upper limits can provide further constraints for models since they give limits in the case of very high luminosity and on short timescales.

4. DISCUSSION

We are reporting here results obtained in the hard X-ray domain (20 to ~ 650 keV) from the first revolution dedicated to V404 Cyg by the *INTEGRAL* mission. While the extreme variability makes it difficult to get instantaneous values of the parameters of emitting region(s), we studied the source evolution during the flaring activity to estimate values representative of the global emission. We have shown that the observed emission can be described with two components. Several scenarios are able to account for the data, but we had to choose one to present the results in a way as instructive as possible. In this work, the first component is identified with a thermal Comptonization emission. The low-energy curvature has required a specific attention. Three parameters can help to describe it properly: an absorbing factor, N_h ; a reflection factor, R ; or the temperature of the seed photons, kT_0 . However, for each of them, the fit procedure converges toward unusual values: N_h of the order of a few $\times 10^{24} \text{ cm}^{-2}$, in contradiction with the soft X-rays observations (Motta et al. 2015), $R \sim 5$, which would imply a peculiar geometry or $kT_0 \sim 7 \pm 1$ keV. This may be linked to the exceptional source luminosity or reflect the presence of another component at low energy or else another origin of the seed photons. The unceasing variability of the Comptonizing population parameters, in space and/or in time, may also be responsible for the observed shape, since any gradient in kT or τ modifies the resulting emission. We give in this paper the results obtained with $kT_0 = 7$ keV. The reflection component is not included since it would add an additional free parameter that cannot be constrained. We have checked that to add a reflection factor (fixed to 1) only slightly modifies the best-fit parameter values and does not affect the scientific conclusions.

For the second component, we have chosen a cutoff power law with a photon index of 1.6 and a cutoff energy of 300 keV to test a scenario similar to that observed in Cyg X-1 (Jourdain et al. 2012).

With the above hypothesis, we obtain a good description of the data and identify two states. (a) A quiet phase, when the source flux remains relatively low (300 mCrab) and the spectrum hard, with a Comptonization temperature ~ 40 keV. (b) An “active” phase, when the source flares, has a huge variability and impressive amplitude changes and a plasma temperature around 25 keV. The second component is not required during the quiet phase and varies significantly during the active phase. Both components contribute to the global flux intensity, even if their variations are not strictly correlated, leading to an evolving spectral shape. This suggests that they are due to two different but probably linked mechanisms.

The similarity between V404 Cyg and Cyg X-1 spectral shapes in the high-energy domain suggests that the second component could be related to a jet contribution extending from radio up to hard X-rays. The radio flaring activity reported during the outburst (Mooley et al. 2015) could be used to test this hypothesis. Polarization measurements could give a decisive answer. However, if the extreme variability of the

source also affects the jet component, it could cancel any coherent polarization signal.

In addition, such an exceptional event requires a careful study of the 500 keV energy domain. In the presented observations, we did not detect any narrow features at 511 keV on the timescales of hours or days. This means that if 511 keV photons are produced, the flux does not exceed $2 \times 10^{-4} \text{ ph cm}^{-2} \text{ s}^{-1}$ (2σ) for a width of 4.5 keV and a total duration of 150 ks.

The large amount of high statistics data from V404 Cyg opens a large domain of new studies: spectral variability over the minute timescale, evolution of the high-energy component, timing studies in the hard X-ray/soft gamma-ray domains, etc. This means that what we will learn from this peculiar event will give us a new view of this family of objects.

5. SUMMARY AND CONCLUSION

The analysis of the V404 Cyg 2015 outburst is still in its early stages. The multiwavelength campaign triggered by the first observations ensures a huge amount of data. The hard X-ray domain enlightens the innermost regions of the source and reveals the behavior of the most energetic particles at work during the flaring activity. The source emission is satisfactorily described by a hot (40–50 keV) Comptonized component, with no need for a second component (“quiet state”), or by a cooler Comptonizing plasma (25–30 keV) plus a second component, possibly related to jet synchrotron emission, which appears above the thermal cutoff (“active state”).

A search for a narrow emission at 511 keV remained unsuccessful, but deeper studies are required to investigate the presence of any broad and/or shifted feature potentially related to the annihilation process.

INTEGRAL has observed this source for four weeks. This will allow the polarization to be investigated. Also, information coming from all wavelengths will have to be correlated to reveal a more complete picture of the source and understand the physics at work. In conclusion, V404 Cyg offers us, with this exceptional outburst, a unique opportunity to make a significant breakthrough in both the X-ray transient phenomenon and X-ray binary systems.

The *INTEGRAL* SPI project has been completed under the responsibility and leadership of CNES. The Italian co-authors acknowledge the Italian Space Agency (ASI) for financial support under ASI/INAF agreement No. 2013-025-R.0. We are grateful to ASI, CEA, CNES, DLR, ESA, INTA, NASA, and OSTC for support.

Note: Results on the two next revolutions are reported in Rodriguez et al. (2015), with a different spectral description. All the SPI spectra presented in our paper are made available in a fits format on the site given in footnote 2 in order to allow anybody to test different models.

REFERENCES

- Arnaud, K. 1996, in ASP Conf. Ser. 101, *Astronomical Data Analysis Software and Systems V*, ed. G. H. Jacoby & J. Barnes (San Francisco, CA: ASP), 17
 Barthelmy, S. D., D’Ai, A., D’Avanzo, P., et al. 2015, *GCN*, 17929, 1
 Casares, J., Charles, P. A., & Naylor, T. 1992, *Natur*, 355, 614
 Jourdain, E., Roques, J. P., M. Chauvin, M., & Clark, D. J. 2012, *ApJ*, 761, 27
 Makino, F. 1989, *IAUC*, 4782, 1
 Miller-Jones, J. C. A., Jonker, P. G., Dhawan, V., et al. 2009, *ApJL*, 706, L230

- Mooley, K., Fender, R., Anderson, G., et al. 2015, ATel, [7658](#)
- Motta, S., Beardmore, A., Oates, S., et al. 2015, ATel, [7665](#)
- Natalucci, L., Flocchi, M., Bazzano, A., et al. 2015, [ApJL](#), [813](#), [L21](#)
- Rodriguez, J., Cadolle Bel, M., & Alfonso-Garzón, J. 2015, [A&A](#), [581](#), [L9](#)
- Roques, J. P., Bouchet, L., Jourdain, E., et al. 1994, [ApJS](#), [92](#), [451](#)
- Roques, J. P., Schanne, S., Von Kienlin, A., et al. 2003, [A&A](#), [411](#), [L91](#)
- Syunyaev, R. A., Kaniovskii, A. S., Efremov, V. A., et al. 1991, SvAL, [17](#), [123](#)
- Teegarden, B. J., & Watanabe, K. 2006, [ApJ](#), [646](#), [965](#)
- Ubertini, P., Lebrun, F., Di Cocco, G., et al. 2003, [A&A](#), [411](#), [L131](#)
- Vedrenne, G., Roques, J. P., Schonfelder, V., et al. 2003, [A&A](#), [411](#), [L63](#)
- Younes, G. A. (on behalf of the Fermi GBM Team) 2015, GCN, 17932, 1